

Localization and delocalization of ultracold bosonic atoms in finite optical lattices

Dirk-Sören Lühmann,¹ Kai Bongs,^{2,3} Klaus Sengstock,² and Daniela Pfannkuche¹

¹*Institut für Theoretische Physik, Universität Hamburg, Jungiusstrasse 9, 20355 Hamburg, Germany*

²*Institut für Laser-Physik, Universität Hamburg, Luruper Chaussee 149, 22761 Hamburg, Germany*

³*Midlands Centre for Ultracold Atoms, School of Physics and Astronomy, University of Birmingham, Edgbaston, Birmingham B15 2TT, United Kingdom*

(Dated: 19 February 2008)

We study bosonic atoms in small optical lattices by exact diagonalization and observe a striking similarity to the superfluid to Mott insulator transition in macroscopic systems. The momentum distribution, the formation of an energy gap, and the pair correlation function show only a weak size dependence. For noncommensurate filling we reveal in deep lattices a mixture of localized and delocalized particles, which is sensitive to lattice imperfections. Breaking the lattice symmetry causes a Bose-glass-like behavior. We discuss the nature of excited states and orbital effects by using an exact diagonalization technique that includes higher bands.

PACS numbers: 03.75.Lm, 03.75.Hh

I. INTRODUCTION

Trapped atoms in optical lattices offer a fantastic new system for applications in quantum optics, quantum information processing, and as a model system for solid state physics. The depth and the shape of the lattice potential, which is proportional to the square of the laser field, can be controlled with great accuracy [1]. Feshbach resonances allow the tuning of the interaction between the neutral atoms in a wide range [2]. As a fascinating new development, experiments with a small number of lattice sites and in particular finite optical chains have become focus of actual research. Prominent examples are quantum registers in the context of quantum information processing [3, 4, 5], the manipulation of single atoms within few sites [6], and experiments with double well unit cells [7]. In this context a fundamental question arises: How similar are finite systems compared with macroscopic systems?

In a macroscopic lattice, bosonic atoms undergo the quantum phase transition from a superfluid phase to a Mott insulator when the depth of the lattice potential is tuned from shallow to deep. This was first discussed for liquid helium on porous media [8], later proposed for neutral repulsively interacting atoms in optical lattices [9], and recently observed experimentally [10, 11, 12]. Driven by the competition of repulsive interaction and kinetic energy the atoms localize on single lattice sites in the Mott insulator phase. Consequently, each site becomes occupied by a fixed integer number of particles leading to a crystal-like situation. In the presence of disorder the system can also undergo a transition to a Bose glass phase [8, 13, 14, 15, 16].

In this article, we study the problem of few repulsively interacting bosonic atoms in finite linear chains and small two-dimensional lattices and discuss how finite size effects influence the precursors of the Mott insulator and the Bose glass transition. The rich physics of the crossover from a double well to mesoscopic systems is investigated by exact diagonalization using a multiband basis, which allows accurate results and the discussion of orbital effects which were widely neglected so far.

We find a surprisingly strong similarity to the localization process in macroscopic systems and show that the pair cor-

relation function is nearly size independent. Moreover, we gain an intuitive insight into the excitation spectrum. Finite systems offer also an unique possibility to study the effects of noncommensurate filling, in which the localization is suppressed by the equivalence of the lattice sites. We observe the formation of an insulating lowest band and in deep lattices we find the coexistence of localized and delocalized atoms. However, these delocalized states are extremely sensitive to lattice imperfections which force the localization of atoms in a Bose-glass-like phase.

II. THEORETICAL MODEL

The short range interaction potential of ultracold bosonic atoms can be approximated by a contact potential $g\delta(\mathbf{r} - \mathbf{r}')$ with the interaction parameter $g = \frac{4\pi\hbar^2}{m}a_s$, where a_s is the s -wave scattering length and m the mass of the atoms [17]. Thus, the Hamiltonian including the full two-particle interaction in a periodic potential V_P is given by

$$\hat{H} = \int d^3r \hat{\psi}^\dagger(\mathbf{r}) \left[\frac{\hat{\mathbf{p}}^2}{2m} + V_P(\mathbf{r}) + \frac{g}{2} \hat{\psi}^\dagger(\mathbf{r}) \hat{\psi}(\mathbf{r}) \right] \hat{\psi}(\mathbf{r}), \quad (1)$$

where $\hat{\psi}(\mathbf{r})$ is the bosonic field operator. We use the potential $V_P = V_{0x} \cos^2(kx) + V_{0y} \cos^2(ky) + V_{0z} \cos^2(kz)$ that is truncated to $(n_x, 1, 1)$ sites for chains and $(n_x, n_y, 1)$ sites for two-dimensional lattices. The periodic potential is continued at its boundary by a harmonic confinement potential [18] (see inset of Fig. 1). We model an optical lattice with the periodicity $a = 515$ nm ($k = \pi/a$) and vary the depth of the lattice from $1E_R$ to $40E_R$ given in units of the recoil energy $E_R = \frac{\hbar^2 k^2}{2m} = 2.16$ h kHz. The quasi-one-dimensional chains and two-dimensional lattices have a transversal confinement $V_{0y} = V_{0z} = 40E_R$ and $V_{0z} = 40E_R$, respectively, so that the transversal tunneling can be neglected. Exact diagonalization is performed in the Bloch representation of the optical lattice. By using a few-particle basis the two-particle interaction is fully included. The truncation of the basis at a sufficiently high energy allows the inclusion of orbital effects [19]. The calculations are performed for ^{87}Rb atoms which are present in many experimental setups.

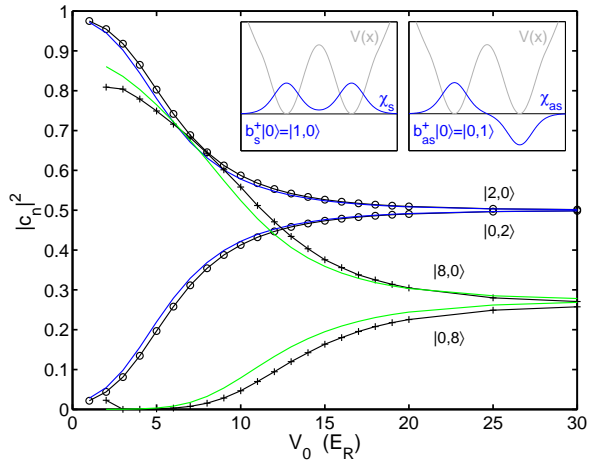


FIG. 1: (Color online) The lowest coefficients c_n for two (\circ) and eight atoms ($+$) in a double well potential in dependency on the lattice depth V_0 calculated by exact diagonalization. The lines without markers are obtained using the LBA. The inset shows a symmetric and an antisymmetric basis wave function.

III. A PRECURSOR OF THE MOTT INSULATOR IN FINITE SYSTEMS

We start the discussion with atoms in a double well which exhibit a crossover reminiscent of the superfluid to Mott insulator transition. Although the double well with commensurate filling represents an intuitive and easy-to-handle model, the eigenstates and the spectrum have already a structure similar to the studied chains with 3 to 10 sites. A double well with two particles can easily be treated analytically with the restriction to the lowest band. The Hilbert space separates into states with even and odd parity that do not couple. The subspace with even parity comprises of the states $|2, 0\rangle = \frac{1}{\sqrt{2}}b_s^{\dagger 2}|0\rangle$ and $|0, 2\rangle = \frac{1}{\sqrt{2}}b_{as}^{\dagger 2}|0\rangle$, where b_s^{\dagger} is the creation operator of particles in the symmetric state and b_{as}^{\dagger} in the antisymmetric state (see inset of Fig. 1). Since the energy difference between symmetric and antisymmetric single-particle states χ_s and χ_{as} is twice the tunneling energy t , the energy of the states $|2, 0\rangle$ and $|0, 2\rangle$ differs by $2\Omega = 4t + \Delta$. The difference in the interaction energies Δ equals $g \int d^3r [\chi_{as}^4(\mathbf{r}) - \chi_s^4(\mathbf{r})]$ using the real space representation. The off-diagonal matrix element between both states is $I = g \int d^3r \chi_s^2(\mathbf{r})\chi_{as}^2(\mathbf{r})$. Thus, the ground state is given by $\Psi_0 = \cos \theta |2, 0\rangle + \sin \theta |0, 2\rangle$, where

$$\theta = \text{atan}\left(\frac{\Omega - \sqrt{\Omega^2 + I^2}}{I}\right). \quad (2)$$

For very shallow lattices, when t approaches infinity, θ vanishes and $\Psi_{0, V_0 \rightarrow 0}$ equals $|2, 0\rangle$, i.e., both particles occupy the energetically lower symmetric one-particle state.

In the limit of deep lattices ($t \rightarrow 0$) the difference between the symmetric and antisymmetric wave function $\chi_s^2(x) - \chi_{as}^2(x)$ vanishes ($\Delta \rightarrow 0$) and θ approaches $-\pi/4$. Consequently, the ground state is given by $\Psi_{0, V_0 \rightarrow \infty} = \frac{1}{\sqrt{2}}|2, 0\rangle - \frac{1}{\sqrt{2}}|0, 2\rangle$. Using the creation operators of a particle in the left

and right well $b_{l/r}^{\dagger} = \frac{1}{\sqrt{2}}(b_s^{\dagger} \pm b_{as}^{\dagger})$ the ground state can be rewritten as $\Psi_{0, V_0 \rightarrow \infty} = b_{l/r}^{\dagger}|0\rangle$ and it becomes obvious that one particle is localized on the left site and one particle on the right site. In addition to the localization, a fundamental property of a Mott-insulator-like state is an excitation gap which is given here by $2I$. The first excited state with an uneven parity and the second excited state $\Psi_{1/2, V_0 \rightarrow \infty} = \frac{1}{2}(b_l^{\dagger 2} \mp b_r^{\dagger 2})|0\rangle$ are degenerate [20]. Both states are symmetric-antisymmetric combinations of doubly occupied sites and thus represent particle-hole excitations. In chains and lattices these linear combinations of particle-hole excitations build up the excited band as discussed further below.

Some of the coefficients c_n in the expansion of the many-body wave function of the ground state are plotted in Fig. 1. Already for a double well it is instructive to compare the results that are obtained using the lowest band approximation (LBA) with numerical multiband calculations. For $V_0 \lesssim 10E_R$ the deviations are well noticeable, whereas in deep lattices the LBA leads to nearly perfect results for filling factor $\nu = 1$. For higher filling factors the total interaction energy and consequently the deviations increase, since higher one-particle bands are occupied in order to minimize the interaction energy. Exemplarily, the coefficients of the states $|8, 0\rangle$ and $|0, 8\rangle$ for filling factor $\nu = 4$ are plotted in Fig. 1. Additionally, the lowest band coefficients $|6, 2\rangle$, $|4, 4\rangle$, and $|2, 6\rangle$ contribute. For higher filling factors than $\nu = 1$ the deviations do not vanish in deep lattices, since in that case ν interacting particles are trapped on each site, leading to a modification of the effective single particle orbitals. This has direct implications for the Bose-Hubbard model [9, 21] which is widely used in this context and is commonly restricted to the lowest band. Figure 1 shows that for higher filling factors ($\nu \gtrsim 3$) this restriction leads to noticeable deviations from a multiband calculation, whereas for low filling factors the deviations are small. Experimentally, deviations for higher fillings have been observed, e.g., by measuring the on-site interaction energy [22, 23].

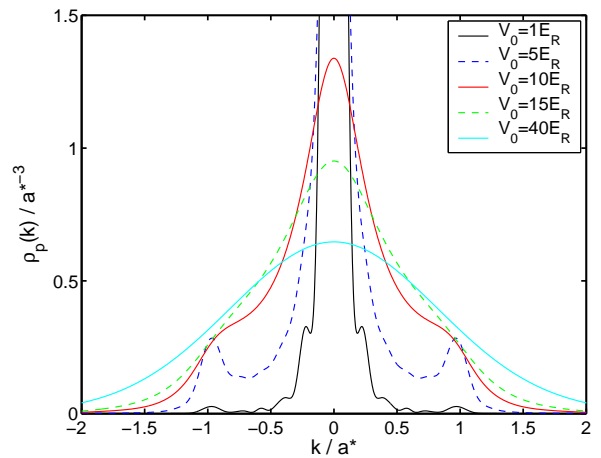


FIG. 2: (Color online) The momentum distribution of six bosons in a quasi-one-dimensional chain with six sites. The crossover from a delocalized wave function ($V_0 \lesssim 5E_R$) to a localized wave function ($V_0 \gtrsim 10E_R$) can be observed.

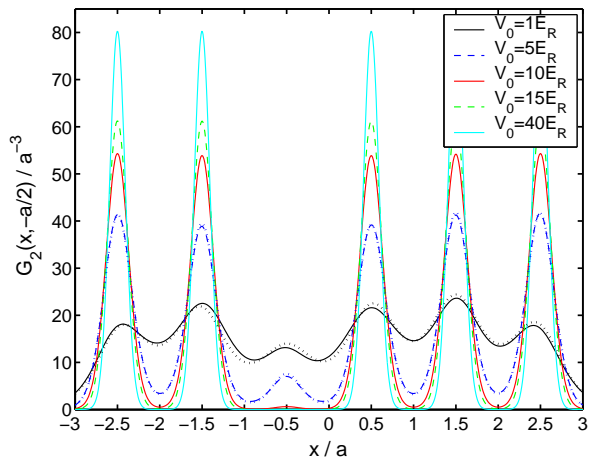


FIG. 3: (Color online) The pair correlation function of six bosons in a chain with six sites shows the localization of particles for $V_0 \gtrsim 10E_R$. Due to the low filling factor $\nu = 1$, the deviation from results obtained using the LBA (dotted lines) are only noticeable for $V_0 \lesssim 5E_R$.

In the following, we extend the double well to a chain with $N_s = 6$ lattice sites and six particles. The momentum distribution $\rho_p(k_x)$ of the chain is shown for different lattice depths V_0 in Fig. 2, where $k_y = k_z = 0$. For very shallow lattices ($V_0 = 1E_R$) a narrow central peak indicates the delocalization of all particles over the lattice, whereas for deep lattices a broad Gaussian momentum distribution is observable. The latter can be assigned to particles that are localized in the center of a single lattice site. Although the system is very small the similarity to macroscopic experimental results [10, 12] is striking. This is a first indication that the localization mechanism is not very size dependent (see also [24]) which is discussed in detail below.

For $V_0 = 1E_R$ minor dips in the momentum distribution (Fig. 2) at $k_n = (n/N_s)a^*$ are observable, where $a^* = 2\pi/a$ is the reciprocal lattice vector. These dips originate from the suppression of standing waves in the confinement with odd parity and wavelengths $\lambda_n = N_s a/n$ with $n = 1, 2, \dots$, since the ground state has an even parity. Increasing the lattice depth to $V_0 = 5E_R$, Bragg peaks located at the reciprocal lattice vector appear. At the same time, the central peak drops rapidly in height and becomes broader, i.e., the particles begin to separate into different wells as the interaction grows relative to the tunneling. At $V_0 = 10E_R$ the minima are smeared out and only a small modulation of momentum density due to delocalized particles remains. This progress proceeds with increasing lattice depth, so that for approximately $V_0 = 30E_R$ the momentum distribution has a Gaussian shape, corresponding to completely localized particles [25].

However, a Gaussian momentum distribution may also arise from a superposition of delocalized states and does not prove the localization on single lattice sites. Therefore, the pair correlation function

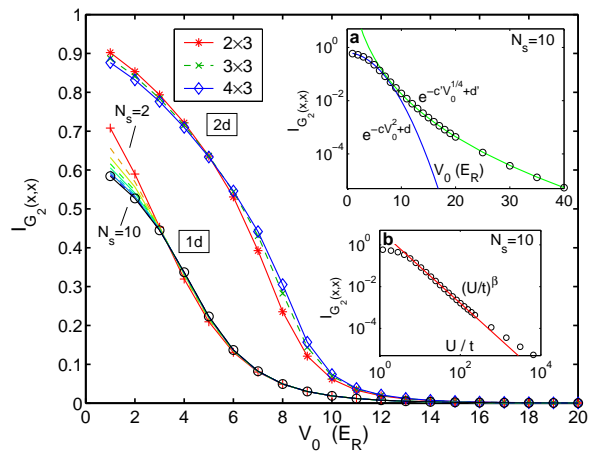


FIG. 4: (Color online) The integral over the local correlation function for chains with N_s sites and small two-dimensional lattices (6, 9, and 12 sites) with filling factor $\nu = 1$ (in LBA). Inset (a) is a logarithmic plot in units of V_0/E_R and inset (b) is a double logarithmic plot in units of U/J for a chain with ten sites.

$$G_2(\mathbf{r}, \mathbf{r}') = \frac{1}{\rho(\mathbf{r}')} \langle \hat{\psi}^\dagger(\mathbf{r}) \hat{\psi}^\dagger(\mathbf{r}') \hat{\psi}(\mathbf{r}') \hat{\psi}(\mathbf{r}) \rangle \quad (3)$$

at $y = z = 0$ is studied, which reflects the conditional density of $N - 1$ particles if one particle can be found at \mathbf{r}' . In Fig. 3 the pair correlation is shown for $x' = -\frac{a}{2}$, i.e., for one particle located on the third site. For $V_0 \lesssim 5E_R$ other particles can be found on the same site, whereas for $V_0 \gtrsim 10E_R$ the pair correlation vanishes on the third site completely. Hence, that site and consequently all sites are occupied with exactly one particle in deep lattices.

The integral over the *local* correlation function $I_{G_2(x,x)} = \frac{N/(N-1)}{\int dx \rho(x)} \int dx G_2(x,x)$ measures the average probability of finding two particles at the same position and is consequently a good measure for the total spatial correlation of particles. In Fig. 4 the local correlation integral is shown for chains with N_s sites and filling factor $\nu = 1$. The calculations are restricted to the lowest band which is quite accurate due to the low filling (see Fig. 3).

Overall we see an exponential decay of the correlation integral with increasing lattice depth. In deep lattices the integral vanishes which reflects the localization of all particles. For $V_0 \lesssim 6E_R$ the correlation decreases with an exponent $-cV_0^2$ [see fit for $N_s = 10$ in the inset (a) of Fig. 4]. Thus, an increase of the potential barriers causes a relatively strong separation of particles in this regime due to the strong overlap of wave functions. For $V_0 \gtrsim 8E_R$ the particles are located predominately on single lattice sites and the extent to neighboring sites is small. In this region the exponential decay is weaker and the correlation drops with an exponent $-c'V_0^{1/4}$. It is remarkable that our calculations show a crossover between two different correlation regimes already for a small sized system.

In the studied systems we observe a partial loss of spatial correlation in the region corresponding to the superfluid phase

as also found in Ref. [24]. Moreover, we see finite correlations above the transition point, which can be understood quantitatively by using a perturbative ansatz to first order in t/U [11, 26], where t is the tunneling matrix element and U the on-site interaction energy. The perturbed wave function can be written as $\Psi' = \Psi_{MI}^{\nu=1} + \frac{t}{U} \sum_{ij} b_i^\dagger b_j \Psi_{MI}^{\nu=1}$ where $\Psi_{MI}^{\nu=1}$ is the pure Mott insulator state at infinite lattice depth which has a vanishing local correlation. The operator $b_i^\dagger b_j$ creates a particle-hole state with a hole on site j and a doubly occupied site i . For doubly occupied sites the pair correlation has a constant value if neglecting the interaction. Hence, the expectation value of the correlation integral is roughly proportional to $(t/U)^2$. In a double-logarithmic plot in units of U/t [inset (b) of Fig. 4] the correlation integral shows a linear behavior between $V_0 = 6E_R$ and $17E_R$, i.e., the integral is proportional to $(U/t)^\beta$. We observe a value for β that is slightly above $\beta = -2$ (about 13%). For shallow lattices the simple perturbative ansatz is obviously not suited and for very deep lattices ($V_0 > 20E_R$) the expectation values are above the power law fit (see also Ref. [11]).

Only in very shallow lattices the correlation integral varies noticeably with the number of lattice sites, whereas for $V_0 > 3E_R$ the integral is nearly size independent (even for a double well system). Additionally, the differences for $V_0 < 3E_R$ are quite small for more than four lattice sites. Thus, the localization of particles depends very weakly on the number of lattice sites N_s , which indicates that the localization may occur in the same manner also in chains of macroscopic size. We conclude that the blocking mechanism, which is caused by the tunneling prohibiting repulsion, is to a large extent insensitive to changes of the system size. Apparently, the coherence length in the insulating region drops below the extend of the system, which becomes consequently a good representation of a larger one. This explains the similarity of the presented momentum distributions and experimental results.

Exemplarily, the energy spectrum of a system with $N_s = 6$ sites, plotted in Fig. 5, shows the formation of narrow many-particle bands for deep lattices. The spectrum is in accordance with the experimentally observed excitation spectrum in Ref. [12]. The bands are gapped by the interaction energy U of two particles on the same site, so that, for example, the first excited band consists of states where one particle interacts on average with one other particle on the same site. The number of states in each band is given by the possibilities to remove a certain number of particles and put them onto other sites resulting in an interaction energy of nU (e.g., the first band has 30 states due to 6 possible sites for a hole and 5 possible sites with double occupation). In particular, the energy of the nondegenerate ground state decreases and the ground state becomes separated from the excited states which is characteristic for an incompressible Mott insulating state. In the limit of deep lattices the interaction energy of the ground state vanishes, since the wave function overlap decreases due to the localization on single sites. The energy of the excited bands slowly increases due to the stronger confinement. Since the sites are equivalent, the eigenstates of the bands are delocalized. These delocalized states that form the excited bands in this commensurate system reappear within the ground-state band of noncommensurate systems, which are discussed in

the next section.

The results obtained so far for momentum distributions, correlation functions, and energy spectra of quasi-one-dimensional chains can be generalized to lattices. As an example, we study a quasi-two-dimensional lattice with 3×3 lattice sites with integer filling factor $\nu = 1$. The momentum distribution is presented in Fig. 6 for different potential depths. It shows the crossover from delocalization to localization and compares well with experimental results [26]. For $5E_R$ and $7.5E_R$ Bragg peaks at $\mathbf{k} = \pm a^* \hat{\mathbf{k}}_x$ and $\mathbf{k} = \pm a^* \hat{\mathbf{k}}_y$ appear in the distribution. Due to the finite number of sites per dimension, additional dips at $k = \frac{\pi}{3} a^*$ can be observed. Increasing the lattice depth, the momentum distribution smears out due to the localization of particles. This starts at approximately $10E_R$ and is far advanced at $12.5E_R$, which is in accordance with the critical point for infinite systems [27]. The two-dimensionality of the system becomes apparent for V_0 between $10E_R$ and $15E_R$. The momentum distribution reflects the square symmetry of the boundary of a single lattice site. At roughly $V_0 = 30E_R$ the distribution becomes a Gaussian which indicates that the particles are located deep in the wells. Then the confining potential experienced by the particles is circular symmetric and can be approximated by a two-dimensional harmonic oscillator, which is reflected in the momentum distribution.

A more detailed picture of the localization process is given by the integral over the local correlation function $I_{G_2(x,x)}$ which is plotted in Fig. 4. Compared with the quasi-one-dimensional chain, the localization process is shifted towards deeper potentials because of two reasons: The interaction energy on each lattice site is diminished due to smaller confinement in the y direction and the tunneling is enhanced since tunneling to four nearest neighbors is possible. For the two-dimensional lattice, we observe the formation of gapped excited bands in deep lattices as well as the separation of the ground state in the energy spectrum in the same way as discussed for chains.

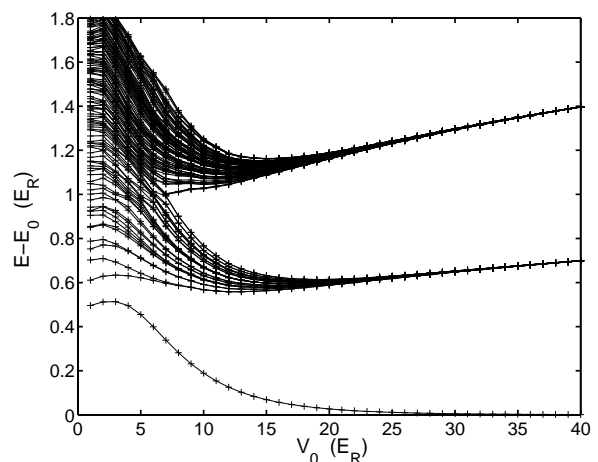


FIG. 5: The energy spectrum of six bosons in a chain with six sites relative to the energy E_0 of the noninteracting system. The spectrum shows the ground state and the two lowest bands.

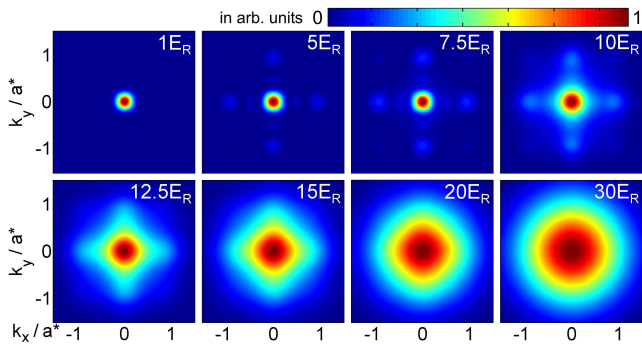


FIG. 6: (Color online) The momentum distribution (normalized to 1) of a two-dimensional 3×3 lattice with nine atoms for various lattice depths V_0 using the LBA.

We are aware that the finite systems discussed here cannot exhibit macroscopic phases and a phase transition. Nonetheless, the precursors to the superfluid phase and the Mott insulator map on many aspects known from macroscopic systems. The momentum distribution (Figs. 2 and 6), the correlation function (Figs. 3 and 4) and the energy spectrum (Fig. 5) show that the localization process is in good agreement with infinite systems. Finite size effects can be observed but do not dominate the behavior of the system. Therefore, simulations with few lattice sites are also quite applicable to larger systems and offer an intuitive and detailed insight due to the accuracy and the inclusion of orbital effects. In the next section we use our method to examine systems with noncommensurate filling.

IV. NONCOMMENSURATE FILLING

When a noncommensurate filling of the lattice is present the physical situation becomes more complicated. The localization of all particles as in the Mott-insulator-like regime is suppressed by the symmetry of the potential, since the equivalence of sites requires the same filling on all sites. Consequently, particles which in principle would prefer localization must delocalize over the whole lattice. The differences to commensurate filling can be illuminated by considering a double well with three atoms restricted to the lowest band. The basis of even parity states comprises of the two states $|3, 0\rangle = \frac{1}{\sqrt{6}}b_s^\dagger|3, 0\rangle$ and $|1, 2\rangle = \frac{1}{\sqrt{2}}b_s^\dagger b_{as}^{\dagger 2}|0\rangle$. The difference in energy between both basis elements is $2\Omega = 4t + \Delta$ with $\Delta = g \int d^3r [\chi_{as}^4(\mathbf{r}) + 4\chi_s^2(\mathbf{r})\chi_{as}^2(\mathbf{r}) - 3\chi_s^4(\mathbf{r})]$ and the off-diagonal matrix element is $I = \sqrt{3}g \int d^3r \chi_s^2(\mathbf{r})\chi_{as}^2(\mathbf{r})$. Thus, the solution for the ground state is given by the same expression as for two particles, i.e., $\Psi_0 = \cos\theta|3, 0\rangle + \sin\theta|1, 2\rangle$. In deep lattices the tunneling energy t vanishes, but Δ , which had vanished for two particles, becomes $4I/\sqrt{3}$.

The ground state in the limit of deep lattices is given by $\Psi_{0, V_0 \rightarrow \infty} = \frac{\sqrt{3}}{2}|3, 0\rangle - \frac{1}{2}|1, 2\rangle = \frac{1}{2}b_l^\dagger b_r^\dagger (b_l^\dagger + b_r^\dagger)|0\rangle$, since θ becomes $2\pi/3$. This represents a wave function with two atoms that are localized and one atom that is delocalized between both wells. Consequently, the ground state is a mixture of localized and delocalized particles. Of great importance in this context is that in this limit the first excited state, which

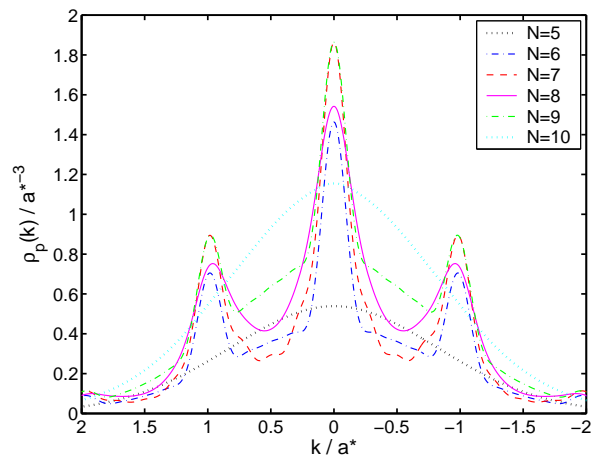


FIG. 7: (Color online) The momentum distribution of $N = 5$ to 10 atoms in a chain with five sites at $V_0 = 40E_R$. For a perfectly symmetric potential the localization of all particles can only be observed at integer filling (dotted lines).

has odd parity and is given by $\Psi_{1, V_0 \rightarrow \infty} = \frac{1}{2}b_l^\dagger b_r^\dagger (b_l^\dagger - b_r^\dagger)|0\rangle$, becomes degenerate with the ground state. Small asymmetries lead to linear combinations of the two quasidegenerate states and result in the nonsymmetric states $\frac{1}{\sqrt{2}}b_l^{\dagger 2} b_r^\dagger|0\rangle$ and $\frac{1}{\sqrt{2}}b_l^\dagger b_r^{\dagger 2}|0\rangle$. Consequently, in a potential with broken symmetry the *third* particle can localize in one of the wells, if the lattice is deep enough. This localization process depends on the potential difference between the two wells compared to the energy difference between ground and first excited state $E_1(V_0) - E_0(V_0)$. The third and fourth excited state which form the "first excited band" are separated from the ground state by $4I/\sqrt{3}$.

These intuitive results for a double well transfer nicely to chains and even two-dimensional lattices. Exemplarily, a chain with $N_s = 5$ sites filled by 5 to 10 particles is studied. The momentum distribution for deep lattices ($V_0 = 40E_R$) obtained by exact diagonalization is shown in Fig. 7. For integer filling factors ($N = 5$ and $N = 10$) a Mott insulator momentum distribution can be observed as discussed in the previous section. When, for example, adding a sixth particle to a chain with filling factor $\nu = 1$, the additional particle cannot localize, since all lattice sites are equivalent. Despite being delocalized at different sites, the particle has a high probability density at the lattice site centers. Therefore, the momentum distribution reflects the lattice structure very clearly. Correspondingly, it shows peaks at 0 and $\pm a^*$ as well as smaller peaks at $\pm na^*$ with $n = 2, 3, \dots$, which originate from the delocalized particles. Additional to this peak structure the momentum distribution has an underlying Gaussian background, which arises from localized particles. Recapitulating the ground state for three particles in a double well $\Psi_{0, V_0 \rightarrow \infty} = \frac{1}{2}b_l^\dagger b_r^\dagger (b_l^\dagger + b_r^\dagger)|0\rangle$, the interpretation is straight forward: For noninteger filling factors ν , the number of particles may be written as $N = \kappa N_s + N_{\text{add}}$ with the corresponding integer filling factor κ and the number of additional particles N_{add} . In deep lattices κN_s particles localize in the wells of the lattice and the remaining N_{add} are delocalized.

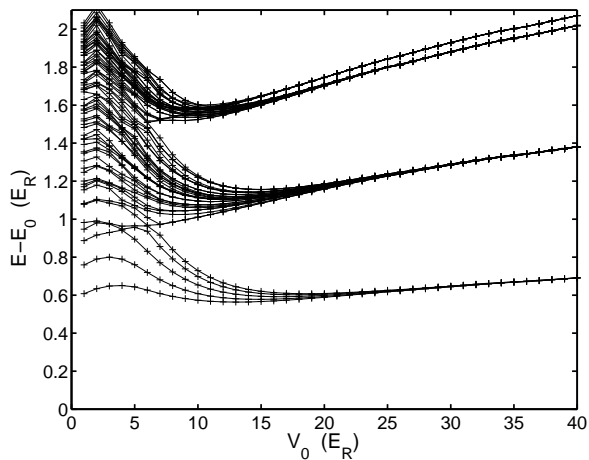


FIG. 8: The energy spectrum for six particles on five sites shows the formation of a lowest many-particle band.

The plotted momentum distribution for $V_0 = 40E_R$ in Fig. 7 shows that for $N = 6$ particles the Gaussian background is noticeably smaller than for five particles. This indicates that the localized particles are influenced by the delocalized hopping particle which experiences the same repulsive interaction on all lattice sites and consequently interacts with all localized particles. For seven particles the height of the peaks increases due to two hopping particles, whereas for eight particles the background increases, since more sites are doubly occupied. Finally, for nine particles all sites except one are doubly occupied which is equivalent to the tunneling of a hole in a lattice with filling $\nu = 2$. We also find the delocalization for noncommensurate filling by analyzing the pair correlation function $G_2(x, x')$ [28].

The energy spectrum for six particles in a chain with $N_s = 5$ sites is shown in Fig. 8. For deep lattices the formation of bands can be observed, which are roughly separated by the two-particle interaction energy U . An interesting feature is the splitting of the second excited band which would not be observable in the LBA. The states with higher energy have three doubly occupied sites whereas the other states have one triply occupied site. Their energy is reduced by a stronger deformation of the wave function accounting for the effective repulsive potential created by the two other atoms at the same site. As seen before for a double well, the ground state becomes quasidegenerate and lies within a band of N_s states. Therefore, the ground state is extremely sensitive to small perturbations of the lattice potential, which is discussed in the next section.

It is hardly surprising that the rich physics of noncommensurate filling can also be found in two-dimensional lattices, including the formation of a lowest band with its discussed implications. For a two-dimensional lattice it is interesting to explore the quantum mechanical nature of the states that are contributing to the lowest band. For a 3×3 lattice with ten particles the lowest band consists of nine states due to the one additional particle in comparison with commensurate filling. Similar to Fig. 8 these states become quasi-degenerate with increasing lattice depth representing all delocalized combinations with the two-particle interaction energy U . In Fig. 9 the

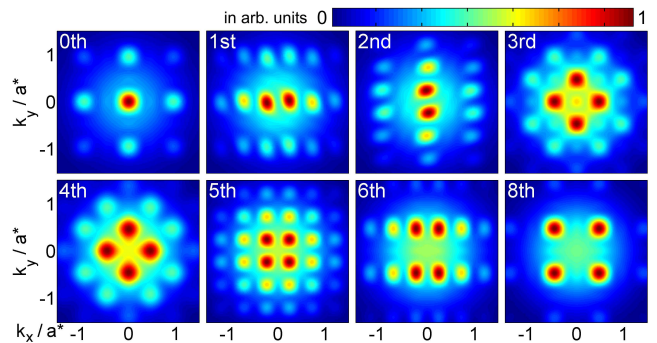


FIG. 9: (Color online) The momentum distribution (normalized to 1) of the lowest band states of a two-dimensional 3×3 lattice with ten atoms at $V_0 = 30E_R$ (in LBA). The seventh excited state, which corresponds to the sixth excited state (rotated by $\pi/2$), is not shown here [29].

momentum distribution of the lowest band states is plotted at $V_0 = 30E_R$ (the seventh state is not shown) [29]. The strong interference pattern of the momentum distribution is in eye-catching contrast with the Gaussian shape of a Mott insulator state and reflects the delocalization. The general structure of the shown band states with only few states can be generalized to larger noncommensurately filled lattices and to particle-hole excitations for commensurate filling.

V. NONCOMMENSURATE FILLING IN A HARMONIC CONFINEMENT

As a last point we discuss the noncommensurate filling under the influence of an additional symmetry-breaking potential. Perturbations of the lowest band states that allow the localization of the additional particles on specific sites. Consequently, a small external confinement can destroy the partly delocalized phase in the same way as small random site offsets caused by lattice fluctuations in a Bose glass [8]. The parameter which triggers the localization of the additional N_{add} particles is the bandwidth of the lowest band which must be similar or smaller than the site offsets to attain localized particles. In experimental setups perfectly flat potentials are hard to achieve, due to the finite waist of the laser beams, which establish the optical lattice, and additional external fields. We investigate this effect by using a chain with five sites and six particles that experience an additional potential $-2V_T e^{-2x^2/w_0^2}$ with $V_T = 40E_R$. The potential is motivated by the Gaussian beam waist w_0 given in units of the lattice constant a , but it can also be approximated by the harmonic potential $\frac{4V_T}{w_0^2}x^2$. The momentum distribution at $V_0 = 20E_R$ is shown in Fig. 10 for different beam widths w_0 ranging from $w_0 = 10a$ to $w_0 = 200a$. The corresponding offset energies relative to the central site are given by $\epsilon_1 = \frac{160}{w_0^2/a^2}E_R$ and $\epsilon_2 = 4\epsilon_1$ (see inset of Fig. 10). The width of the ground state band at $V_0 = 20E_R$ is roughly $\frac{1}{50}E_R$.

In order to localize the additional particle, the offset ϵ_1 is important with respect to the bandwidth. For $w_0 = 200a$ and $w_0 = 120a$ peaks due to delocalization can be well identified

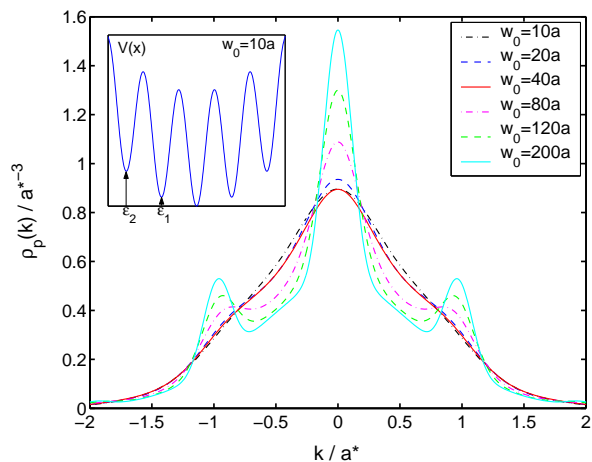


FIG. 10: (Color online) The momentum distribution of six atoms in a chain with five sites at $V_0 = 20E_R$ for a laser beam with a finite Gauss width w_0 . The inset shows the corresponding site offsets ϵ_1 and ϵ_2 .

in the momentum distribution, but at $w_0 = 80a$ ($\epsilon_1 = \frac{1}{40}E_R$) this structure is smeared out. At $w_0 = 40a$ ($\epsilon_1 = \frac{1}{10}E_R$) the momentum distribution matches the distribution for commensurate filling shown in Fig. 2 (at $V_0 \approx 15E_R$), i.e., the sixth particle is localized in the center of the lattice. Below $w_0 = 40a$ the momentum distribution does not change noticeably. Instead, the *density* changes drastically, since the gain in potential energy ϵ_2 exceeds the repulsive interaction of two particles at the same site U . At $w_0 = 20a$ the density at the two outer sites vanishes and the inner sites are doubly occupied, due to a total energy gain of roughly $2(\epsilon_2 - U) \approx 2 \times (1.6E_R - 0.6E_R)$. For the stronger confinement $w_0 = 10a$ the central site is even occupied by four particles.

Despite the harmonic potential the lattice symmetry can be broken by applying different moderate perturbation potentials (such as single site offsets or a linear potential). The localization process remains qualitatively the same for the studied finite systems, since basically local site offsets are responsible for the localization. We conclude that in perturbed lattices a Bose-glass-like localization of all particles can always be achieved in sufficiently deep lattices triggered by the ratio of offset energies and bandwidth. However, in intermediate lattices a mixed phase with N_{add} delocalized particles can be observed, if the lattice fluctuations are smaller than the bandwidth. Increasing the lattice depth (decreasing the bandwidth) first κN_s particles and in deeper potentials the remaining N_{add} particles localize. Experimentally the observation of the mixed phase

may be hindered by the finite temperature of the BEC. We note that in stronger harmonic confinements in which the offset energies match the interaction energy U ($w_0 \lesssim 20a$ for the system above) a precursor of a shell structure can be observed, which shows regions with different occupations per site [30].

VI. CONCLUSIONS

We have studied bosonic atoms in finite optical lattices using an exact treatment which includes effects of higher bands. Due to the equivalence of sites, finite lattices with integer filling factors exhibit a fundamentally different behavior than those with noninteger filling factors. The well studied superfluid to Mott insulator transition can be recovered in finite commensurately filled chains and two-dimensional lattices with few lattice sites. Our results show the localization of atoms in deep lattices and reveal a striking similarity to the momentum distribution observed in macroscopic systems. Furthermore, we have shown that the local correlation is widely independent of the system size which indicates that the localization process in small systems compares with that in infinite systems. The localization is also reflected by the formation of an energy gap in the energy spectrum.

For noninteger filling factors only the particles that correspond to integer filling localize in deep lattices whereas the additional particles are delocalized. The coexistence of localized and delocalized particles in the ground state can be observed in the momentum distribution and the pair correlation function. The energy spectrum shows the formation of a narrow lowest band in deep lattices causing the ground state to be extremely sensitive to perturbations of the potential such as lattice imperfections or additional confinements. Triggered by the ratio of bandwidth and site offsets one observes the localization of all particles which is similar to the localization process in a Bose glass. In weakly confined systems this leads to a localization which occurs in deeper potentials than in lattices with commensurate filling.

Briefly, we have shown how the macroscopic physics of the Mott insulator and of the Bose glass transfer to finite systems and that the detailed simulation of small systems offer important information about larger ones. Especially, we gained detailed insight into the localization behavior of experimentally relevant finite systems.

VII. ACKNOWLEDGMENTS

We thank Frank Deuretzbacher for valuable discussions.

-
- [1] P. Jessen and I. Deutsch, *Adv. Atom., Mol., Opt. Phys.* **37**, 95 (1996).
 - [2] S. Inouye, M. R. Andrews, J. Stenger, H.-J. Miesner, D. M. Stamper-Kurn, and W. Ketterle, *Nature (London)* **392**, 151 (1998).
 - [3] D. Jaksch, H.-J. Briegel, J. I. Cirac, C. W. Gardiner, and P. Zoller, *Phys. Rev. Lett.* **82**, 1975 (1999).
 - [4] G. K. Brennen, C. M. Caves, P. S. Jessen, and I. H. Deutsch, *Phys. Rev. Lett.* **82**, 1060 (1999).
 - [5] D. Schrader, I. Dotsenko, M. Khudaverdyan, Y. Miroshnychenko, A. Rauschenbeutel, and D. Meschede, *Phys. Rev. Lett.* **93**, 150501 (2004).
 - [6] Y. Miroshnychenko, W. Alt, I. Dotsenko, L. Förster, M. Khudaverdyan, D. Meschede, D. Schrader, and A. Rauschenbeutel,

- Nature (London) **442**, 151 (2006).
- [7] J. Sebby-Strabley, M. Anderlini, P. S. Jessen, and J. V. Porto, Phys. Rev. A **73**, 033605 (2006).
- [8] M. P. A. Fisher, P. B. Weichman, G. Grinstein, and D. S. Fisher, Phys. Rev. B **40**, 546 (1989).
- [9] D. Jaksch, C. Bruder, J. I. Cirac, C. W. Gardiner, and P. Zoller, Phys. Rev. Lett. **81**, 3108 (1998).
- [10] M. Greiner, O. Mandel, T. Esslinger, T. W. Hänsch, and I. Bloch, Nature (London) **415**, 39 (2002).
- [11] F. Gerbier, A. Widera, S. Fölling, O. Mandel, T. Gericke, and I. Bloch, Phys. Rev. Lett. **95**, 050404 (2005).
- [12] T. Stöferle, H. Moritz, C. Schori, M. Köhl, and T. Esslinger, Phys. Rev. Lett. **92**, 130403 (2004).
- [13] B. Damski, J. Zakrzewski, L. Santos, P. Zoller, and M. Lewenstein, Phys. Rev. Lett. **91**, 080403 (2003).
- [14] L. Fallani, J. E. Lye, V. Guarrera, C. Fort, and M. Inguscio, Phys. Rev. Lett. **98**, 130404 (2007).
- [15] R. Pugatch, N. Bar-gill, N. Katz, E. Rowen, and N. Davidson, e-print arXiv:cond-mat/0603571 (2006).
- [16] R. T. Scalettar, G. G. Batrouni, and G. T. Zimanyi, Phys. Rev. Lett. **66**, 3144 (1991).
- [17] A. J. Leggett, Rev. Mod. Phys. **73**, 307 (2001).
- [18] The confining potential $V(x) = \gamma V_{0x} \left(\frac{2kx}{n\pi}\right)^2$ continues the periodic potential at $|x| = x_0$, where n is the number of sites. The potential is continuously differentiable which determines γ (≈ 1) and x_0 ($\approx na/2$).
- [19] We used up to 100 000 basis states and parity conservation if applicable including the formed Bloch bands and the lowest "continuum" states (bound states in the confinement).
- [20] The first excited state $\Psi_1 = |1, 1\rangle = b_s^\dagger b_{as}^\dagger |0\rangle$ remains unchanged and the second excited state is given by $\Psi_2 = \cos \theta' |2, 0\rangle + \sin \theta' |0, 2\rangle$ with $\theta' = \text{atan}[(\Omega + \sqrt{\Omega^2 + I^2})/I]$.
- [21] D. Jaksch and P. Zoller, Ann. Phys. (N.Y.) **315**, 52 (2005).
- [22] We can confirm the experimental observation and the calculation in Ref. [23] also by the diagonalization of several bosons on a single site. The on-site energy U of filling factor $\nu = 5$ is, e.g., roughly 17% smaller than for $\nu = 1$ at $V_0 = 30E_R$.
- [23] G. K. Campbell, J. Mun, M. Boyd, P. Medley, A. E. Leanhardt, L. G. Marcassa, D. E. Pritchard, and W. Ketterle, Science **313**, 649 (2006).
- [24] R. Roth and K. Burnett, Phys. Rev. A **67**, 031602(R) (2003).
- [25] The density on one site corresponds to the density of a single particle in a single-sited \cos^2 potential, but deviates slightly from the harmonic approach.
- [26] I. B. Spielman, W. D. Phillips, and J. V. Porto, Phys. Rev. Lett. **98**, 080404 (2007).
- [27] N. Elstner and H. Monien, Phys. Rev. B **59**, 12184 (1999).
- [28] Additional information can be obtained from the pair correlation function $G_2(x, x')$ in deep lattices with one particle fixed in the middle of a specific site. As seen before, the correlation vanishes at that site for filling factor $\nu = 1$. For noninteger filling ($6 \leq N \leq 9$) the height of the correlation function varies for each site. Thus, regarding the integer number of particles, at least some particles must be delocalized between the sites.
- [29] The first and second excited state, the third and fourth excited state as well as the sixth and seventh excited state are exactly degenerate.
- [30] G. G. Batrouni, V. Rousseau, R. T. Scalettar, M. Rigol, A. Muramatsu, P. J. H. Denteneer, and M. Troyer, Phys. Rev. Lett. **89**, 117203 (2002).